

Reconciliation of halogen-induced ozone loss with the total-column ozone record

Article

Accepted Version

Shepherd, T. G., Plummer, D. A., Scinocca, J. F., Hegglin, M. I., Fioletov, V. E., Reader, M. C., Remsberg, E., von Clarmann, T. and Wang, H. J. (2014) Reconciliation of halogen-induced ozone loss with the total-column ozone record. *Nature Geoscience*, 7 (6). pp. 443-449. ISSN 1752-0908 doi: <https://doi.org/10.1038/NGEO2155> Available at <https://centaur.reading.ac.uk/36861/>

It is advisable to refer to the publisher's version if you intend to cite from the work. See [Guidance on citing](#).

Published version at: <http://www.nature.com/ngeo/journal/v7/n6/full/ngeo2155.html>

To link to this article DOI: <http://dx.doi.org/10.1038/NGEO2155>

Publisher: Nature Publishing Group

All outputs in CentAUR are protected by Intellectual Property Rights law, including copyright law. Copyright and IPR is retained by the creators or other copyright holders. Terms and conditions for use of this material are defined in the [End User Agreement](#).

www.reading.ac.uk/centaur

CentAUR

Central Archive at the University of Reading

Reading's research outputs online

Reconciling halogen-induced ozone loss with the observed total ozone record

T.G. Shepherd^{1*}, D.A. Plummer², J.F. Scinocca², M.I. Hegglin¹, V.E. Fioletov³, M.C.
Reader⁴, E. Remsberg⁵, T. von Clarmann⁶, H.J. Wang⁷

¹Department of Meteorology, University of Reading, Reading RG6 6BB, U.K.

²Canadian Centre for Climate Modelling and Analysis, Environment Canada,
Victoria, British Columbia V8W 3V6, Canada

³Environment Canada, 4905 Dufferin St., Toronto, Ontario M3H 5T4, Canada

⁴School of Earth and Ocean Sciences, University of Victoria, P.O. Box 3055, Victoria,
British Columbia V8W 3P6, Canada

⁵National Aeronautics and Space Administration, Langley Research Center,
Hampton, VA 23681-2199 U.S.A.

⁶Institute for Meteorology and Climate Research, Karlsruhe Institute of Technology,
D-76021 Karlsruhe, Germany

⁷School of Earth and Atmospheric Sciences, Georgia Institute of Technology, Atlanta,
GA 30332-0340 U.S.A.

*e-mail: theodore.shepherd@reading.ac.uk

Second revised version, March 2014

1 **The observed depletion of the ozone layer is attributed to anthropogenic**
2 **halogens, but the precision of this attribution is complicated by natural**
3 **dynamical variability (year-to-year meteorological variations) and by changes**
4 **in tropospheric ozone, leaving key aspects of the observed total ozone record**
5 **unexplained. These include inter-hemispheric differences in the response to**
6 **the Mount Pinatubo volcanic eruption, the lack of a decline prior to 1980 and**
7 **of any long-term decline in the tropics, and the apparent delay in ozone**
8 **recovery despite the significant decline of stratospheric halogen loading since**
9 **the late 1990s. Here we use a chemistry-climate model constrained by**
10 **observed meteorology to remove the effects of dynamical variability and to**
11 **estimate changes in tropospheric ozone. Ozone loss is shown to closely follow**
12 **stratospheric halogen loading, with pronounced enhancements in both**
13 **hemispheres following the volcanic eruptions of El Chichon and, especially,**
14 **Mount Pinatubo. Approximately 40% of the long-term non-volcanic loss is**
15 **found to have occurred by 1980. Long-term ozone loss is found in the tropical**
16 **stratosphere, but is masked in the column by tropospheric increases. Ozone**
17 **loss has declined by over 10% since stratospheric halogen loading peaked in**
18 **the late 1990s, indicating that recovery of the ozone layer is well underway.**

19
20 Anthropogenic emissions of halogenated (principally chlorine) species have led to
21 an observable depletion of the ozone layer¹. Ozone depletion has been a matter of
22 wide public concern because of its implications for human and ecosystem health².
23 As a result of comprehensive controls on ozone-depleting substances, stratospheric

1 chlorine loading peaked in the late 1990s and has been slowly declining since then¹,
2 and is expected to continue to decline over the coming decades. Observed total
3 ozone levels have been stable since the late 1990s, rather than showing the expected
4 increase, but there is large year-to-year dynamical variability which can plausibly
5 obscure the onset of ozone recovery^{1,3}.

6

7 Understanding the observed ozone record is important not only for confirming the
8 efficacy of the Montreal Protocol but also for testing the physical understanding of
9 ozone depletion. This becomes especially pertinent since ozone recovery will take
10 place in the presence of climate change, which affects the ozone layer through both
11 dynamical and chemical mechanisms⁴. For example, surface ultraviolet radiation
12 may not only be affected by halogen-induced ozone depletion but also by ozone
13 changes resulting from climate change⁵. From this perspective, it is important to
14 resolve several outstanding puzzles in the observed ozone record, e.g.: (i) Given that
15 stratospheric aerosol is expected to enhance halogen-induced ozone loss⁶, why was
16 there no decline in total ozone levels following the Mount Pinatubo eruption in the
17 Southern Hemisphere (SH), only in the Northern Hemisphere (NH)¹? (ii) Why has
18 there been no observed decline in tropical total ozone¹, in contrast with model
19 simulations⁷ and in spite of observed ozone decreases in the stratosphere⁸? (iii) Why
20 did total ozone only decline after about 1980¹, given that stratospheric halogen
21 loading reached about 40% of its maximum in 1980⁹ and again in contrast to model
22 simulations⁴?

23

1 The combined ground-based and satellite record provides a reliable measure of
2 global total column ozone changes since 1964¹⁰. About 90% of total ozone resides in
3 the stratosphere, so it is generally assumed that the total ozone record can be
4 interpreted in terms of stratospheric changes¹. Attribution of the observed
5 depletion of total ozone to anthropogenic halogens is complicated by internal
6 dynamical variability of the climate system, natural external forcing from solar
7 variability and volcanoes, and possible effects of climate change. Furthermore,
8 tropospheric ozone is believed to have increased through the 20th century as a result
9 of increased anthropogenic emissions of ozone precursors^{11,12,13}, and this could have
10 affected the total ozone record. Indeed the globally averaged tropospheric ozone
11 increases since pre-industrial times are estimated to be comparable in magnitude to
12 the halogen-induced stratospheric ozone decreases¹⁴. However, reliable
13 observational estimates of long-term changes in tropospheric ozone on a global
14 scale do not exist.^{12,13}

16 **Combining models and measurements**

17 To quantify halogen-induced ozone loss in a changing and variable atmosphere, it is
18 necessary to remove the effects of those changes and variations. This is generally
19 done statistically¹⁵, but not all atmospheric variability is represented in statistical
20 models, the relationships between proxies and ozone are only approximate, and the
21 parameterized effects on ozone are not necessarily separable. Furthermore the
22 effects of secular changes such as climate change or changes in tropospheric ozone
23 are difficult to deal with in such an approach. As a result, statistical estimates of

halogen-induced loss can depend sensitively on the period chosen and the statistical model used¹⁶, especially in the tropics and NH where ozone depletion is comparatively small relative to the SH, and the effect of other factors comparatively large.

However it is well known that stratospheric ozone is slaved to the meteorology, once the source gases are prescribed¹⁷. Furthermore, stratospheric ozone chemistry is well established, with generally good agreement concerning chemical mechanisms between chemistry-climate models and measurements¹⁸. (See Methods for discussion of the model used here.) This means that the effect of chemical perturbations, such as halogen loading, on ozone changes can be determined by reproducing the ozone changes with a chemistry-climate model driven by the observed meteorology, using known chemical processes, and then calculating the difference in ozone between simulations performed with and without the chemical perturbation¹⁹.

The success of such an approach relies on being able to reproduce the past changes, which in turn relies on having a sufficiently good estimate of the past meteorology. Previous attempts have had difficulty reproducing the past ozone changes because of deficiencies in the meteorological reanalyses used to drive the model¹⁹. Developments in data assimilation have recently led to much more stable reanalyses. We use the ERA-Interim reanalysis²⁰ covering the period 1979-2009 to drive a chemistry-climate model (see Methods). The ERA-40 reanalysis²¹ is used to

1 examine the pre-1979 period. This introduces an inhomogeneity in the modelled
2 timeseries, which is bridged using the run with constant ozone depleting substances
3 (cODS) as a transfer standard (see Supplementary Information). The quantification
4 of halogen-induced ozone loss is insensitive to this bridging, since it is computed
5 from the differences between the two simulations.

6
7 In the absence of reliable observational estimates of long-term changes in global
8 tropospheric ozone, estimates are generally derived from models driven by
9 historical estimates of ozone precursor emissions⁹. Such model-based estimates of
10 tropospheric ozone changes are evidently rather uncertain, in part because the
11 emissions are not known very precisely. However, by including those changes
12 within the same modelling framework as that used to simulate the stratospheric
13 ozone changes, a self-consistent estimate of total ozone changes is obtained.
14 Moreover the stratospheric component of those changes can be compared with the
15 more limited observational record available from limb-sounding satellite
16 instruments²². When considered together with the total ozone measurements, this
17 allows inferences to be drawn about the realism of the modelled tropospheric ozone
18 changes, and the contributions of the various factors to the observed total ozone
19 record.

20 21 **Understanding the observed total ozone record**

22 Figure 1 shows timeseries of total ozone anomalies, relative to the 1964-1978
23 reference period, for the near-global mean, SH and NH midlatitudes, and tropics. In

1 general the simulated total ozone including effects of ODS changes (ODS simulation,
2 black) follows the observations (orange) closely, in both year-to-year variability and
3 long-term changes. This level of agreement provides confidence that these
4 simulations can be used to remove the effects of dynamical variability and quantify
5 the halogen-induced ozone loss. Apart from some isolated periods where the
6 variability does not match (mid 1970s for NH midlatitudes, around 1970 for the
7 tropics), which likely indicate issues with the ERA-40 reanalysis, the main
8 discrepancy is that the model under-represents the extent of the long-term decline
9 in NH midlatitudes. The positive model bias in NH midlatitudes is already present in
10 the early 1980s and is fairly stable through to about 2005. This suggests that it is not
11 the result of too little halogen-induced loss, since any such bias would follow the
12 stratospheric halogen loading which peaked in the late 1990s.

13
14 Since springtime polar ozone loss can influence midlatitude ozone²³, springtime
15 polar total ozone is shown for completeness in Figure 2. Whilst the long-term
16 decline is well simulated in the Arctic, the model underestimates the long-term
17 decline in the Antarctic by about 30 DU, or roughly 25% of the total observed
18 depletion. This might be due to the fact the model does not include any
19 representation of Nitric Acid Trihydrate (NAT) polar stratospheric clouds (PSCs) or
20 the associated denitrification²⁴, which has been argued to have a negligible vortex-
21 wide effect in the Arctic²⁵ but to account for about 25% of the depth of the Antarctic
22 ozone hole²⁶. The absence of VSLs bromine in the model could also contribute to the
23 underestimation of Antarctic ozone loss. Since approximately 50% of the observed

1 SH midlatitude annual-mean ozone depletion is believed to result from the ozone
2 hole²³, a 25% underestimation of Antarctic depletion implies a 10-15%
3 underestimation of SH midlatitude depletion. As will be seen (e.g. Table 1), this
4 corresponds to the actual extent of underestimation found here (about 11%) but in
5 any case is well within the statistical uncertainties of our quantification.

6

7 The blue curves in Figure 1 (and Figure 2) show the cODS simulation, which exhibits
8 the same interannual variability as the ODS simulation, as well as a long-term
9 increase in total ozone up to about 1980 in NH midlatitudes, and a somewhat
10 smaller increase up to the mid 1980s in the tropics (and thus also in near-global
11 ozone). The timing, magnitude and hemispheric asymmetry of these increases is
12 consistent with increases in tropospheric ozone simulated by chemistry-climate
13 models forced by historical estimates of tropospheric ozone precursor emissions²⁷,
14 and Table 1 confirms that the increases in the cODS simulation primarily occur in
15 the troposphere.

16

17 The ODS-induced ozone loss is determined from the difference between the blue
18 and black curves in Figure 1 and shows, as expected, that the observed long-term
19 ozone decline is attributable to ODS changes. The difference is shown explicitly in
20 Figure 3, together with the modelled stratospheric halogen loading, represented by
21 Equivalent Stratospheric Chlorine (ESC)⁷. In contrast to the large year-to-year
22 variability in ozone itself (Figure 1), the ODS-induced ozone loss is a much smoother
23 function of time and follows the halogen loading closely, modulated by volcanic

aerosol in both hemispheres. Although the full nonlinearity of known stratospheric ozone chemistry is represented in the model, the approximately linear dependence of ozone loss on ESC found here, together with the very close match between ESC and Equivalent Effective Stratospheric Chlorine (EESC)²⁸ which is based on tropospheric halocarbon abundances, supports the use of EESC as an explanatory variable in statistical analyses of global ozone changes²⁹. However Figure 3 also emphasizes the need to include volcanic enhancements in both hemispheres. The ozone loss is seen to be greater (by 50%) in the SH than in the NH, to be enhanced by volcanic aerosol by both El Chichon and, especially, Mount Pinatubo in both hemispheres, to have reached approximately 40% of its maximum (neglecting years influenced by volcanoes) by 1980, and to have occurred in the tropics. All this is consistent with physical understanding, but only the first of these conclusions is evident from the total ozone record (Figure 1) alone. The percentage of the long-term non-volcanic ODS-induced loss incurred by 1980 is quantified in Figure 3 by the 1978-1982 and 1996-2002 mean values, and is $49 \pm 16\%$ in the tropics, $43 \pm 15\%$ in NH midlatitudes, $35 \pm 8\%$ in SH midlatitudes, and $42 \pm 12\%$ globally (see Supplementary Information for calculation of 95% confidence intervals).

The ODS-induced ozone loss computed here does not include possible ozone changes induced by dynamical feedbacks. Any such changes would be apparent in the cODS simulation, which however exhibits no long-term change in stratospheric ozone in any region (Table 1).

1 The interannual variability in total ozone seen in Figure 1 can lead to significant
2 deviations from the ODS-induced behaviour. The strong dip in SH midlatitude ozone
3 in the mid-1980s is also seen in the cODS simulation, showing that it resulted from
4 meteorological variability. The same conclusion applies to the large increase from
5 the late 1990s to the mid-2000s (see also Refs. 30,31). The lack of a decrease in SH
6 midlatitude ozone following the Mount Pinatubo volcanic eruption in 1991 is
7 explained by the fact that chemical loss was masked by a dynamically driven
8 increase, evident in the cODS simulation (see also Refs. 32,33). Although total ozone
9 anomalies are, within the year-to-year variability, fairly stable in all regions since
10 halogen loading peaked in the late 1990s¹, the ODS-induced loss in Figure 3 shows a
11 decline from 1996-2002 to 2006-2009 of $15\pm6\%$ in the tropics, $11\pm9\%$ in NH
12 midlatitudes, $12\pm7\%$ in SH midlatitudes, and $13\pm6\%$ globally, all of which are
13 consistent with the observed decline in stratospheric halogen loading over this
14 period¹.

15
16 In principle there may be a chemical component to the interannual variability, since
17 dynamical variations affect lower stratosphere ozone and temperature in the same
18 way³⁴, e.g. a stronger poleward mass flux implies more extratropical ozone from
19 enhanced transport but also higher temperatures, which reduce ODS-induced ozone
20 loss associated with polar processes. This effect is quantified by the ratio of total
21 ozone anomalies in the ODS to the cODS simulation, during a period of stable
22 halogen loading (Figure 4). A slope exceeding unity indicates chemical amplification
23 of dynamically induced ozone variability. Such an effect is clearly seen in springtime

1 polar-cap averaged ozone levels in the Antarctic, with a much weaker effect
2 apparent in Arctic springtime. However little if any effect is found at midlatitudes.
3
4 In order to reconcile the estimates of ODS-induced long-term ozone loss with the
5 observed total ozone record, it is necessary to consider not only meteorological
6 variability but also the effect of the tropospheric ozone increases apparent in the
7 cODS simulation (blue curves in Figure 1). Although there are no reliable
8 observational estimates of global tropospheric ozone changes, global observations
9 of stratospheric ozone are available from limb-sounding satellite instruments since
10 about 1980²² and can be used as an independent test of model performance. Figure
11 5 shows timeseries of tropospheric and stratospheric partial columns from the ODS
12 simulation, together with the observed stratospheric partial columns. The reference
13 level for the observed anomalies is defined to match the mean value of the modelled
14 anomalies during the MIPAS period (2005-2009), when the observational sampling
15 is most dense, with no further adjustment applied; hence the changes in the
16 observed anomalies relative to MIPAS arise purely from the observations. The
17 modelled stratospheric timeseries are seen to match the monthly-mean variations
18 in the MIPAS record extremely well, providing confidence in the simulated
19 stratospheric partial columns. Good agreement is also found with the SAGE II
20 record, except in the tropics in the late part of the record. Although the earliest
21 estimates from LIMS and SAGE I are noisy, on the whole the comparison with
22 observations suggests that the simulated changes in stratospheric ozone are
23 realistic in all three regions.

1

2 The simulated long-term changes in both stratospheric and tropospheric ozone,
3 between the reference period 1964-1978 and the period 1996-2002 of maximum
4 (non-volcanic) ODS-induced ozone loss, are shown in Table 1 for the ODS and cODS
5 simulations and for their difference. From Table 1 and Figure 5 the following
6 conclusions can be drawn. In SH midlatitudes, the long-term decline in the ODS
7 simulation matches the observed total ozone decline of about 19 DU (6%) and
8 approximately equals the ODS-induced ozone loss. There is a small non-ODS
9 induced increase in tropospheric ozone (3 DU) that is offset by an ODS-induced
10 tropospheric ozone decline, leading to very little net change in tropospheric ozone.

11

12 In NH midlatitudes, the long-term decline in the ODS simulation of 7 DU significantly
13 under-estimates the observed total ozone decline of 12 DU (3%). Because the
14 modelled stratospheric decline of 12 DU is consistent with the observed
15 stratospheric decline, this implies that the modelled tropospheric increase of 5 DU
16 over this period is too large, hence that the assumed emissions of tropospheric
17 ozone precursors increase too much during this period. This is consistent with a
18 general high bias in present-day NH tropospheric ozone in models³⁵. Pre-1980
19 ozone loss was primarily obscured by dynamical variability (note the lack of a
20 discernible trend before 1980 in the modelled stratospheric ozone in Fig. 5b), but
21 also was likely offset to some extent by increases in tropospheric ozone.

22

1 In the tropics, the barely discernible long-term decline in total column ozone in the
2 ODS simulation matches the observations, whilst the decline of 5 DU in the
3 stratosphere, which is attributable to ODS, also matches the observations. Although
4 there is no way of independently confirming the modelled increase of 3 DU in
5 tropospheric ozone, this result shows that the observed total ozone record in the
6 tropics is not necessarily incompatible with observed estimates of a stratospheric
7 ozone decrease, potentially resolving the apparent discrepancy between the two
8 records^{1,8}. The implication is that the ODS-induced ozone decline in the tropics,
9 which is expected from models⁷, was largely masked by increases in tropospheric
10 ozone.

12 **Conclusions**

13 A chemistry-climate model, representing the combined effects of tropospheric and
14 stratospheric ozone chemistry and driven by observed meteorology, has been used
15 to quantify halogen-induced ozone loss and its contribution to the observed total
16 ozone record. Constraining the model by the observed meteorology allows removal
17 of the effects of dynamical variability in a more precise way than is possible using
18 purely statistical methods, while modelling tropospheric ozone together with
19 stratospheric ozone allows investigation of the contribution of tropospheric ozone
20 changes to the observed total ozone record. This approach resolves several
21 outstanding puzzles in that record and allows the identification of the onset of total
22 ozone recovery.

1 Year-to-year variability in ozone mainly arises from meteorological variability
2 together with enhancement of halogen-induced loss from volcanic aerosol loading.
3 The latter is seen to arise in both hemispheres, especially after the eruption of
4 Mount Pinatubo when halogen loading was high, but the chemical impact of Mount
5 Pinatubo on SH midlatitude total ozone was masked by dynamical variability.
6 Variability obscured the fact that approximately 40% of the (non-volcanic) long-
7 term ozone loss had already occurred by 1980. Following the peak stratospheric
8 halogen loading in the late 1990s, variability has similarly obscured a clearly
9 identifiable decline in ODS-induced ozone loss of more than 10%, consistent with
10 the decline in halogen loading, indicating that recovery of the ozone layer is well
11 underway.

12

13 Although emissions of tropospheric ozone precursors are somewhat uncertain and
14 there are no reliable estimates of global changes in tropospheric ozone, the realism
15 of the model simulation of tropospheric ozone changes can be assessed using the
16 independent constraints provided by the observed global record of total ozone
17 (since 1964) and of stratospheric ozone (since 1979). Considered together with the
18 model simulations, these records suggest that the lack of an observed decrease in
19 tropical total ozone is because increases in tropospheric ozone masked the
20 stratospheric ODS-induced decline, reconciling the apparent discrepancy between
21 observed changes in stratospheric and total column tropical ozone. Detailed
22 comparison of nudged simulations as used here with tropospheric ozone
23 measurements may help resolve the conflicting trends apparent in those data sets¹.

1
2
3
4
5
6
7
8
9
10
11
12
13
14
15
16
17
18
19
20
21
22
23

These results show the value of using models and observations together to understand the observed total ozone record, allowing much stronger conclusions than can be obtained from models or observations separately.

Methods

Model simulations. The chemistry-climate model is a version of the Canadian Middle Atmosphere Model (CMAM)³⁶, with 71 vertical levels spanning the surface to about 100 km at a horizontal spectral resolution of T47, corresponding to a 3.75° horizontal grid. Extensive evaluation against observations has shown that CMAM is one of the best performing models in terms of stratospheric transport and chemistry^{1,18}. The chemical kinetics are based on JPL-2006³⁷. Stratospheric source gases (halocarbons, N₂O and CH₄) are prescribed as time-varying tropospheric concentrations, except in the cODS simulation where the halocarbons (but not N₂O or CH₄) are held constant at 1960s values. The halocarbons in the ODS simulation follow the adjusted A1 scenario²³, and do not include any additional bromine or chlorine from VSLS. The absence of halogenated VSLS could lead to an underestimation of ODS-induced ozone loss in polar regions and in midlatitudes during conditions of enhanced aerosol loading²³. The greenhouse gases evolve following the SRES A1B scenario³⁸.

This version of CMAM includes a representation of CH₄-NO_x chemistry within the troposphere, and was included in the Atmospheric Chemistry and Climate Model

1 Intercomparison Project (ACCMIP). Tropospheric chemical forcings were as
2 specified in ACCMIP²⁷. Although the model neglects non-methane volatile organic
3 compounds (NMVOCs), it produces present-day tropospheric ozone levels that
4 compare well with observations, and both pre-industrial and present-day
5 tropospheric ozone levels fall well within the ACCMIP model distribution³⁵. This is
6 consistent with model sensitivity studies which attribute most of the increase in
7 tropospheric ozone since pre-industrial times to the increase in CH₄ and NO_x, with
8 only a minor contribution from NMVOCs³⁹. Thus the model is well designed for
9 investigating changes in the large-scale distributions of tropospheric and
10 stratospheric ozone.

11
12 This version of CMAM is run in a 'specified dynamics' mode, where the
13 meteorological fields (winds and temperature, but not water vapour) at altitudes
14 below 1 hPa are nudged (i.e. relaxed) towards a meteorological reanalysis, with the
15 nudging tapering off rapidly for altitudes above 10 hPa (e.g. nudging strength at 5
16 hPa is 20% of that at 10 hPa). Details of the nudging procedure are provided in Ref.
17 40, except that here the zonal-mean nudging was also tapered off above 10 hPa.
18 Prior to 1979, the model was nudged to the ERA-40 reanalysis²¹ and after 1979 to
19 ERA-Interim²⁰. This introduces an inhomogeneity into the nudged data set across
20 the 1979 transition, which is dealt with as discussed in the Supplementary
21 Information.

22
23 The ozone in the nudged model cannot be expected to follow the observed record

1 exactly, because of uncertainties both in the ozone observations and in the
2 reanalysis used to drive the model, the fact the model will not follow the reanalysis
3 exactly because of the nudging methodology, and model limitations including
4 transport, spatial resolution of low temperature regions, and treatment of chemistry
5 (including PSCs).

6
7 **Observational data sets.** The total column ozone data set is an update of that in
8 Ref. 10, which has been widely used in recent WMO/UNEP Ozone Assessments^{1,23}.
9 Zonal-mean total ozone time series are obtained from ground-based measurements
10 by Dobson and Brewer spectrophotometers and filter ozonometers for the period
11 from 1964 to 2010, using satellite measurements to correct for climatological
12 sampling biases in the ground-based network. The data set has been shown to
13 successfully reproduce seasonal means and averages over longer periods on the
14 global scale¹⁰ as well as springtime variations in polar regions⁴¹. Because solar
15 variability was not included in the model simulations, its effects were removed
16 statistically from the observational timeseries.

17
18 The stratospheric partial column data sets are calculated from the monthly zonal
19 mean ozone climatologies provided by the SPARC Data Initiative²², by integrating
20 the ozone abundances above the zonal mean thermal tropopause, which is
21 calculated from the 3D model temperature fields using the WMO standard
22 tropopause definition⁴² and interpolated onto the SPARC Data Initiative latitude
23 grid. The instruments considered here are LIMS⁴³, SAGE I⁴⁴, SAGE II⁴⁵, and MIPAS⁴⁶.

No attempt is made to remove the effect of the solar cycle from these observations because of the gaps in the record. Note that MIPAS data are only used after January 2005 (version V5R_O3_220), when the instrument switched measurement mode and subsequently showed excellent agreement with SAGE II. An exception to this agreement is the tropical lower stratosphere, where MIPAS compares well to most of the other SPARC Data Initiative climatologies, but not to SAGE II which is biased low in this region²². The latter finding offers a potential explanation of why the stratospheric partial column ozone from SAGE II shows slightly more negative anomalies than the ODS simulation in the tropics in the late 1990s and early 2000s (Figure 5c). Note also that the LIMS version 6 data used here have a known low bias in the tropical lower stratosphere⁴⁷, which may affect the stratospheric partial columns in the tropics.

References

1. World Meteorological Organization, *Scientific Assessment of Ozone Depletion: 2010*, Global Ozone Research and Monitoring Project Report 52 (WMO, 2011).
2. United Nations Environment Programme, *Environmental Effects of Ozone Depletion: 2010 Assessment* (UNEP, 2010).
3. Kieseewetter, G., Sinnhuber, B. M., Weber, M. & Burrows, J. P. Attribution of stratospheric ozone trends to chemistry and transport: a modelling study. *Atmos. Chem. Phys.* **24**, 12073–12089 (2010).

- 1 4. Shepherd, T. G. Dynamics, stratospheric ozone, and climate change. *Atmos.-Ocean*
2 **46**, 371–392 (2008).
- 3 5. Hegglin, M. I. & Shepherd, T. G. Large climate-induced changes in UV index and
4 stratosphere-to-troposphere ozone flux. *Nature Geosci.* **2**, 687–691 (2009).
- 5 6. Solomon, S. *et al.* The role of aerosol variations in anthropogenic ozone depletion
6 at northern midlatitudes. *J. Geophys. Res.* **101**, 6713–6727 (1996).
- 7 7. Eyring, V. *et al.* Multi-model projections of stratospheric ozone in the 21st century.
8 *J. Geophys. Res.* **112**, D16303, doi:10.1029/2006JD008332 (2007).
- 9 8. Randel, W. J. & Wu, F. A stratospheric ozone profile data set for 1979-2005:
10 Variability, trends, and comparisons with column ozone data. *J. Geophys. Res.* **112**,
11 D06313, doi:10.1029/2006JD007339 (2007).
- 12 9. Cionni, I. *et al.* Ozone database in support of CMIP5 simulations: results and
13 corresponding radiative forcing. *Atmos. Chem. Phys.* **11**, 11267–11292 (2011).
- 14 10. Fioletov, V. E., Bodeker, G. E., Miller, A. J., McPeters, R. D. & Stolarski, R. Global
15 and zonal total ozone variations estimated from ground based and satellite
16 measurements: 1964-2000. *J. Geophys. Res.* **107**, 4647, doi:10.1029/2001JD001350
17 (2002).
- 18 11. Lamarque, J.-F. *et al.* Tropospheric ozone evolution between 1890 and 1990. *J.*
19 *Geophys. Res.* **110**, D08304, doi:10.1029/2004JD005537 (2005).
- 20 12. Marenco, A., Gouget, H., Nédélec, P., Pagés, J.-P. & Karcher, F. Evidence of a long-
21 term increase in tropospheric ozone from Pic du Midi data series: Consequences:
22 Positive radiative forcing. *J. Geophys. Res.*, **99**, 16617–16632 (1994).

- 1 13. Parrish, D. D. *et al.* Long-term changes in lower tropospheric baseline ozone
2 concentrations at northern mid-latitudes. *Atmos. Chem. Phys.*, **12**, 11485–11504
3 (2012).
- 4 14. Reader, M. C., Plummer, D. A., Scinocca, J. F. & Shepherd, T. G. Contributions to
5 20th century total column ozone change from halocarbons, tropospheric ozone
6 precursors, and climate change. *Geophys. Res. Lett.* **40**, 6276–6281 (2013).
- 7 15. Mäder, J. A. *et al.* Statistical modeling of total ozone: Selection of appropriate
8 explanatory variables. *J. Geophys. Res.*, **112**, D11108, doi:10.1029/2006JD007694
9 (2007).
- 10 16. Vyushin, D. I., Fioletov, V. E. & Shepherd, T. G. Impact of long-range correlations
11 on trend detection in total ozone. *J. Geophys. Res.* **112**, D14307,
12 doi:10.1029/2006JD008168 (2007).
- 13 17. Hadjinicolaou, P., Pyle, J. A., Chipperfield, M. P. & Kettleborough, J. A. Effect of
14 interannual meteorological variability on mid-latitude O₃. *Geophys. Res. Lett.* **24**,
15 2993–2996 (1997).
- 16 18. Stratospheric Processes And their Role in Climate, *SPARC Report on the*
17 *Evaluation of Chemistry-Climate Models*, V. Eyring, T. G. Shepherd, D. W. Waugh
18 (Eds.), SPARC Report No. 5, WCRP-132, WMO/TD-No. 1526 (SPARC CCMVal, 2010).
- 19 19. Feng, W., Chipperfield, M. P., Dorf, M., Pfeilsticker, K. & Ricaud, P. Mid-latitude
20 ozone changes: studies with a 3-D CTM forced by ERA-40 analyses. *Atmos. Chem.*
21 *Phys.*, **9**, 2357–2369 (2007).
- 22 20. Dee, D. P. *et al.* The ERA-Interim reanalysis: configuration and performance of
23 the data assimilation system. *Q. J. Roy. Meteor. Soc.* **656**, 553–597 (2011).

- 1 21. Uppala, S. M. *et al.* The ERA-40 re-analysis. *Q. J. Roy. Meteor. Soc.* **612**, 2961–3012
2 (2005).
- 3 22. Tegtmeier, S. *et al.* The SPARC Data Initiative: A comparison of ozone
4 climatologies from international limb satellite sounders. *J. Geophys. Res.* **118**,
5 12,229–12,247 (2013).
- 6 23. World Meteorological Organization, Scientific Assessment of Ozone Depletion:
7 2006, Global Ozone Research and Monitoring Project Report 50 (WMO, 2007).
- 8 24. Plummer, D. A., Scinocca, J. F., Shepherd, T. G., Reader, M. C. & Jonsson, A. I.
9 Quantifying the contributions to stratospheric ozone changes from ozone depleting
10 substances and greenhouse gases. *Atmos. Chem. Phys.* **10**, 8803–8920 (2010).
- 11 25. Wegner, T. *et al.* Heterogeneous chlorine activation on stratospheric aerosols
12 and clouds in the Arctic polar vortex. *Atmos. Chem. Phys.* **12**, 11095–11106 (2012).
- 13 26. Portmann, R. W. *et al.* Role of aerosol variations in anthropogenic ozone
14 depletion in the polar regions. *J. Geophys. Res.* **101**, 22991–23006 (1996).
- 15 27. Lamarque, J.-F. *et al.* Historical (1850–2000) gridded anthropogenic and biomass
16 burning emissions of reactive gases and aerosols: Methodology and application.
17 *Atmos. Chem. Phys.* **10**, 7017–7039 (2010).
- 18 28. Newman, P. A., Daniel, J. S., Waugh, D. W. & Nash, E.R. A new formulation of
19 equivalent effective stratospheric chlorine (EESC). *Atmos. Chem. Phys.* **7**, 4537–4552
20 (2007).
- 21 29. Stolarski, R. S., Douglass, A. R., Steensrud, S. & Pawson, S. Trends in stratospheric
22 ozone: Lessons learned from a 3D Chemical Transport Model. *J. Atmos. Sci.* **63**,
23 1029–1041 (2006).

- 1 30. Hadjinicolaou, P., Pyle, J. A. & Harris, N. R. P. The recent turnaround in
2 stratospheric ozone over northern middle latitudes: A dynamical modeling
3 perspective. *Geophys. Res. Lett.* **32**, 12821, doi:10.1029/2005GL022476 (2005).
- 4 31. Dhomse, S., Weber, M., Wohltmann, I., Rex, M. & Burrows, J. P. On the possible
5 causes of recent increases in northern hemispheric total ozone from a statistical
6 analysis of satellite data from 1979 to 2003. *Atmos. Chem. Phys.* **6**, 1165–1180
7 (2006).
- 8 32. Telford, P., Braesicke, P., Morgenstern, O. & Pyle, J. Reassessment of causes of
9 ozone column variability following the eruption of Mount Pinatubo using a nudged
10 CCM. *Atmos. Chem. Phys.* **9**, 4251–4260 (2009).
- 11 33. Poberaj, C. S., Staehelin, J. & Brunner, D. Missing stratospheric ozone decrease at
12 Southern Hemisphere middle latitudes after Mount Pinatubo: A dynamical
13 perspective. *J. Atmos. Sci.* **68**, 1922–1945 (2011).
- 14 34. Randel, W. J. & Cobb, J. B. Coherent variations of monthly mean total ozone and
15 lower stratospheric temperature. *J. Geophys. Res.* **99**, 5433–5447 (1994).
- 16 35. Young, P. J. *et al.* Pre-industrial to end 21st century projections of tropospheric
17 ozone from the Atmospheric Chemistry and Climate Model Intercomparison Project
18 (ACCMIP). *Atmos. Chem. Phys.* **13**, 2063–2090 (2013).
- 19 36. Scinocca, J., McFarlane, N. A., Lazare, M., Li, J. & Plummer, D. Technical
20 Note: The CCCma third generation AGCM and its extension into the middle
21 atmosphere. *Atmos. Chem. Phys.* **8**, 7055–7074 (2008).

- 1 37. Sander, S. P. *et al.* Chemical Kinetics and Photochemical Data for Use in
2 Atmospheric Studies, Evaluation Number 15. JPL Publication 06-2 (Jet Propulsion
3 Laboratory, Pasadena, 2006).
- 4 38. Intergovernmental Panel on Climate Change. Special Report on Emissions
5 Scenarios: A Special Report of Working Group III of the Intergovernmental Panel
6 on Climate Change (Cambridge Univ. Press, 2000).
- 7 39. Shindell, D. T. *et al.* Improved attribution of climate forcing to emissions. *Science*
8 **326**, 716–718 (2009).
- 9 40. McLandress, C., Scinocca, J. F., Shepherd, T. G., Reader, M. C. & Manney, G. L.
10 Dynamical control of the mesosphere by orographic and non-orographic gravity
11 wave drag during the extended northern winters of 2006 and 2009. *J. Atmos. Sci.* **70**,
12 2152–2169 (2013).
- 13 41. Weber, M. *et al.* Stratospheric Ozone, in “State of the Climate in 2011”. *Bull. Amer.*
14 *Meteor. Soc.* **93** (7), S46–S49 (2012).
- 15 42. World Meteorological Organization, *Meteorology – A three-dimensional science.*
16 *WMO Bull*, **6**, 134–138 (WMO, 1957).
- 17 43. Remsberg, E. *et al.* On the quality of the Nimbus 7 LIMS version 6 ozone for
18 studies of the middle atmosphere. *J. Quant. Spectros. Rad. Transf.* **105**, 492–1031
19 (2007).
- 20 44. Wang, H. J., Cunnold, D. M. & Bao, X. A critical analysis of Stratospheric Aerosol
21 and Gas Experiment ozone trends. *J. Geophys. Res.* **101**, 12495–12514 (1996).

45. Wang, H. J., Cunnold, D. M., Thomason, L. W., Zawodny, J. M. & Bodeker, G. E.
Assessment of SAGE version 6.1 ozone data quality. *J. Geophys. Res.* **107**, 4691,
doi:10.1029/2002JD002418 (2002).
46. Von Clarmann, T. *et al.* Retrieval of temperature, H₂O, O₃, HNO₃, CH₄, N₂O,
ClONO₂ and ClO from MIPAS reduced resolution nominal mode limb emission
measurements. *Atmos. Meas. Techn.* **2**, 159–175 (2009).
47. Remsberg, E. *et al.* On the inclusion of Limb Infrared Monitor of the Stratosphere
version 6 ozone in a data assimilation system. *J. Geophys. Res.* **118**, 7982–8000,
doi:10.1002/jgrd.50566 (2013).
48. Stolarski, R. S. & Frith, S. M. Search for evidence of trend slow-down in the long-
term TOMS/SBUV total ozone data record: the importance of instrument drift
uncertainty. *Atmos. Chem. Phys.* **6**, 4057–4065 (2006).
49. Fioletov, V. E. & Shepherd, T.G. Seasonal persistence of midlatitude total ozone
anomalies. *Geophys. Res. Lett.* **30**, 1417, doi:10.1029/2002GL016739 (2003).

Correspondence and request for materials should be addressed to T.G.S.

Acknowledgements

This work was funded by the Canadian Space Agency through the CMAM20 project,
with additional institutional support from the Canadian Centre for Climate
Modelling and Analysis who provided the model code and supercomputing time.

1 **Author contributions**

2 T.G.S. conceived the experiment, interpreted the results, and wrote the paper; D.A.P.
3 performed the diagnostic analysis and devised the bias-correction procedure; J.F.S.
4 devised and implemented the nudging procedure used to perform the experiments;
5 M.I.H. performed the analysis of stratospheric partial column ozone and contributed
6 to the writing; V.E.F. processed and provided the ground-based data and
7 contributed to the interpretation; M.C.R. performed the simulations; and E.R., T.v.C.
8 and H.J.W. processed and provided the LIMS, MIPAS and SAGE data, respectively.

9

10 **Additional information**

11 Supplementary information is provided.

12

13 **Competing financial interests**

14 The authors declare no competing financial interests.

15

16

1 **Figure legends**

2 **Figure 1 | Time evolution of global total ozone.** Deseasonalized total ozone
3 anomalies relative to the 1964-1978 reference period for the model simulation with
4 changing ODS abundances (ODS, black), the model simulation with ODS abundances
5 held constant at 1960s values (cODS, blue), and ground-based observations
6 (orange), for different latitude bands. The model simulations are not plotted across
7 the ERA-40/ERA-Interim transition (see Supplementary Information). The
8 correlation between the ODS simulation and observations over the 1995-2009 time
9 period, during which the halogen loading was not changing rapidly, is indicated
10 within each panel.

11

12 **Figure 2 | Time evolution of polar springtime total ozone.** Total ozone anomalies
13 relative to the 1964-1978 reference period for the model simulation with changing
14 ODS abundances (ODS, black), the model simulation with ODS abundances held
15 constant at 1960s values (cODS, blue), ground-based observations (orange), and
16 satellite observations (TOMS⁴⁸, red), for NH polar cap average in March and SH
17 polar cap average in October. The model simulations are not plotted across the ERA-
18 40/ERA-Interim transition (see Supplementary Information). Since the satellite
19 observations only date from 1979, the mean value of the satellite record over the
20 1979-2009 time period is adjusted to match the mean value of the ground-based
21 record.

22

Figure 3 | Time evolution of halogen-induced ozone loss. Annual-mean column ozone difference between the ODS and the cODS simulation (black dots) for the different latitude bands; negative values correspond to ODS-induced loss. The numbers indicate the average differences, with 95% uncertainties (see Supplementary Information), over 1978-1982, 1996-2002, and 2006-2009. The red curve shows the (inverted) lower stratospheric abundance of Equivalent Stratospheric Chlorine (ESC)⁷ at 50 hPa, consisting of the sum of inorganic chlorine Cly and 60 times inorganic bromine Bry in the model and representing a measure of stratospheric halogen loading, while the blue curve is a smoothed version of the red curve where a 1-2-1 smoother has been applied 10 times to the annual-mean values. The orange curve shows the Equivalent Effective Stratospheric Chlorine (EESC), which is derived directly from tropospheric halocarbon abundances based on the method of Ref 28, using the same multiplier of 60 for bromine and assuming a mean age of 3 years in the tropics and 5 years in midlatitudes.

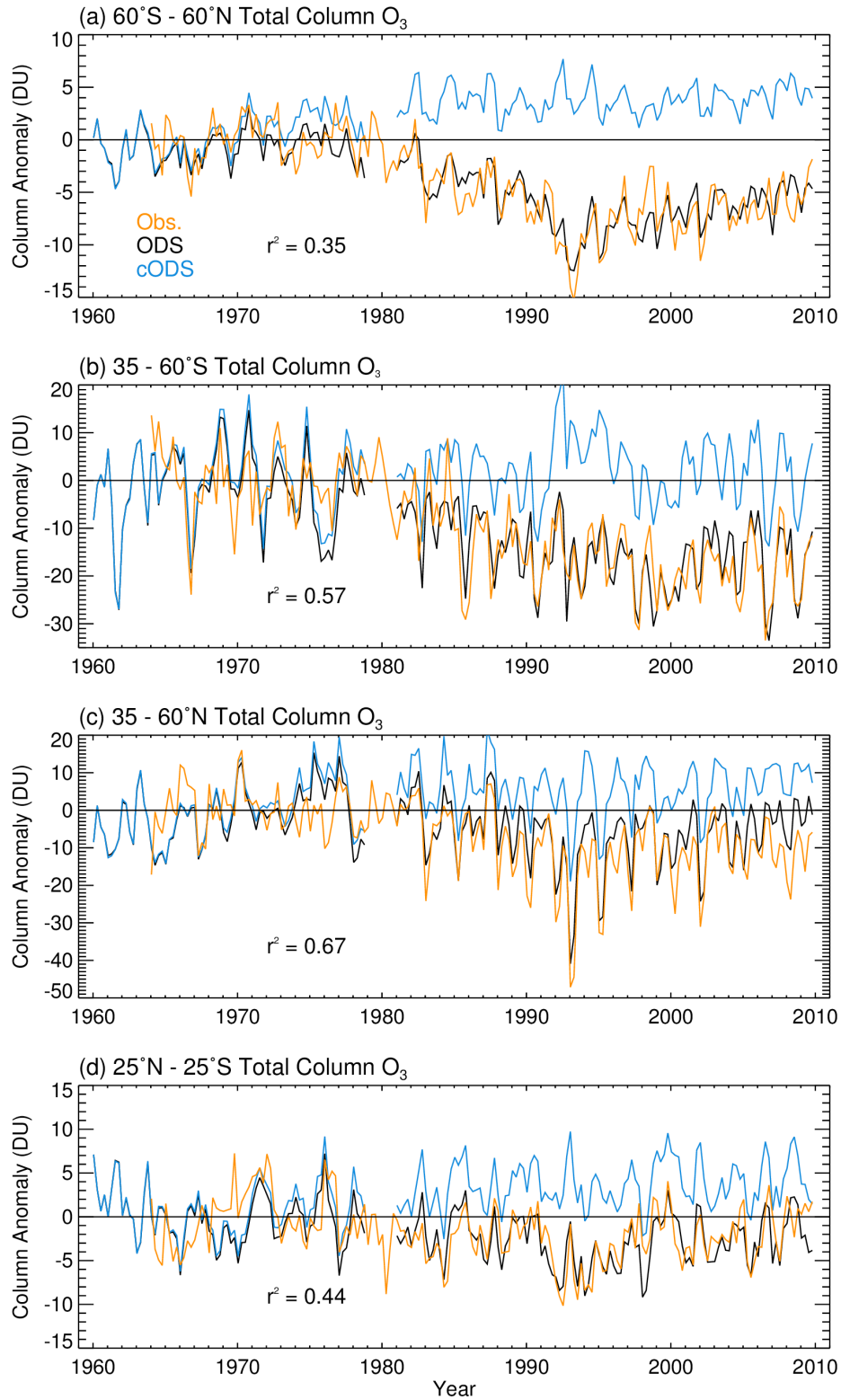
Figure 4 | Quantification of chemical amplification of total ozone variability. Scatterplots of total ozone anomalies from the ODS and cODS simulation over the period 1995-2009 during which the halogen loading was not changing rapidly, for the latitude bands and months indicated. For midlatitudes, the range of months is chosen to match the period of coherent interannual variability, as defined by the persistence of observed midlatitude total ozone anomalies⁴⁹. For polar regions, the range of months corresponds to the spring season.

Figure 5 | Comparison of stratospheric partial column ozone changes with observations. Modelled monthly mean stratospheric (grey) and tropospheric (black) partial column ozone anomalies with respect to the 1964-1978 reference period for the ODS simulation, averaged over different latitude bands. The midlatitude averages are only taken to 55 degrees latitude because the measurement coverage deteriorates rapidly poleward of that latitude. The model simulations are not plotted across the ERA-40/ERA-Interim transition (see Supplementary Information). The coloured lines and dots indicate stratospheric partial column ozone derived from the SPARC Data Initiative monthly zonal mean ozone climatologies³⁵ of LIMS, SAGE I, SAGE II, and MIPAS. The anomalies of the observed data sets are defined such that the mean value of the data matches that from the model during the 2005-2009 (MIPAS) reference period, when the observational sampling is most dense.

Table legend

Table 1 | Quantified long-term ozone changes. Differences are shown between the 1964-1978 and 1996-2002 averages, with declines indicated as negative changes. The percentage changes are with respect to the 1964-1978 climatological mean values. 95% confidence intervals include uncertainties in the mean value over each time period as well as, for the simulations, the uncertainties in the offset applied between the ERA-40 and ERA-Interim portions of the simulation (see Supplementary Information).

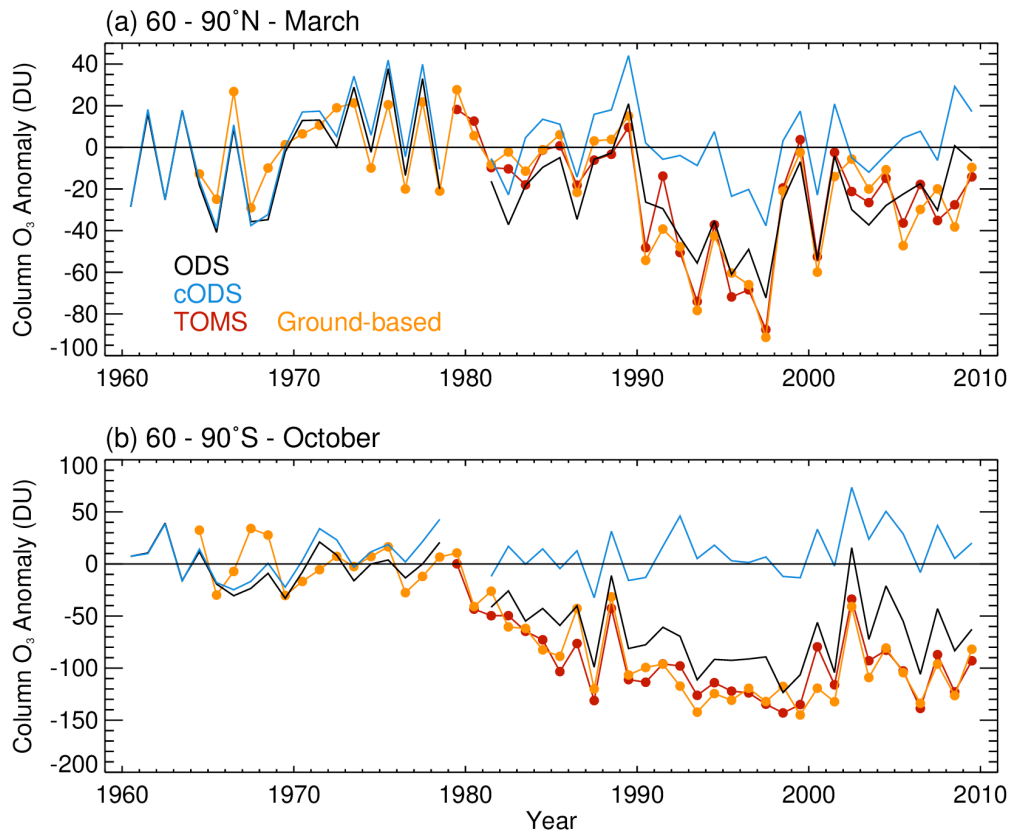
1 **Figure 1**



2

3

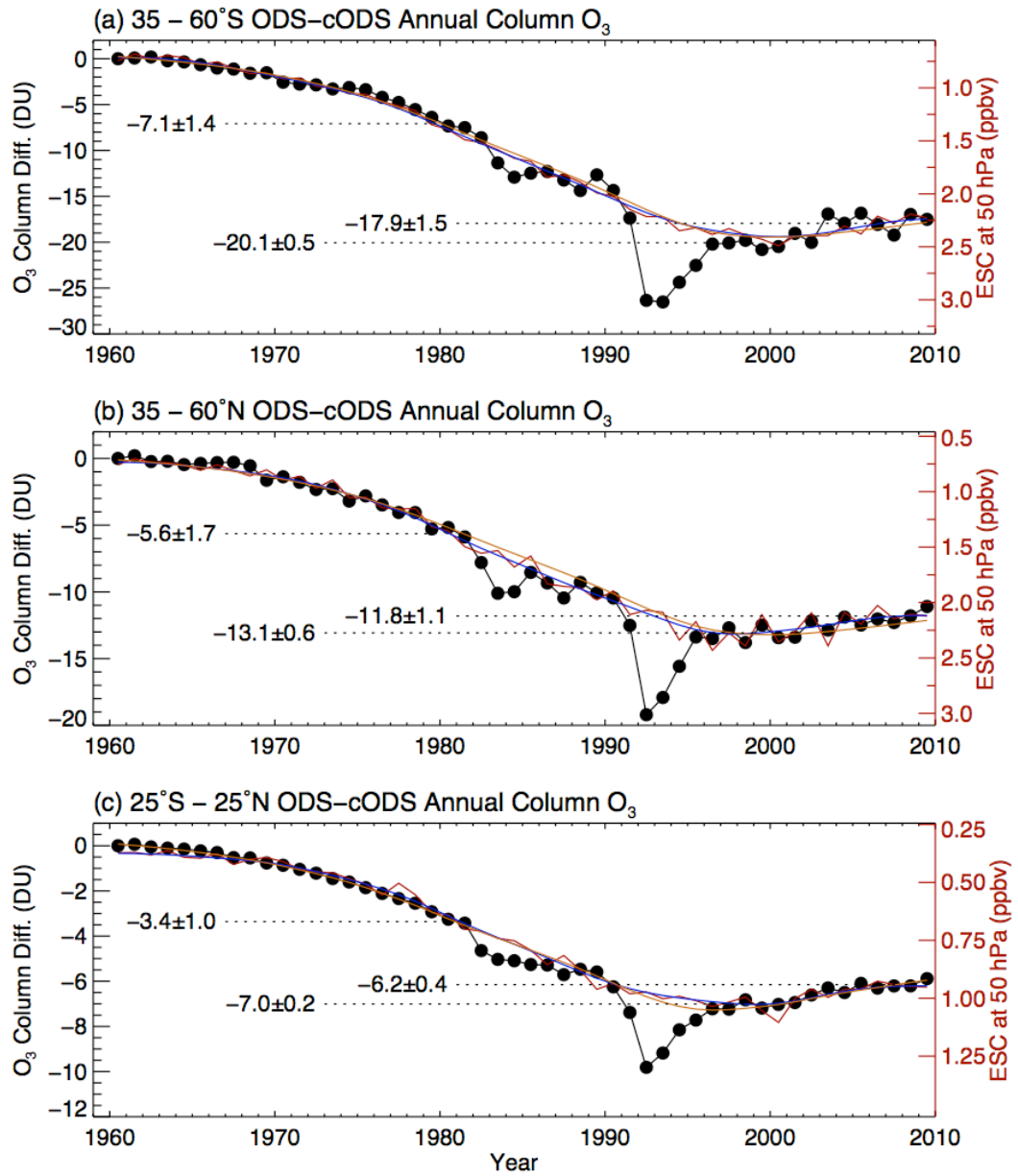
1 **Figure 2**



2

3

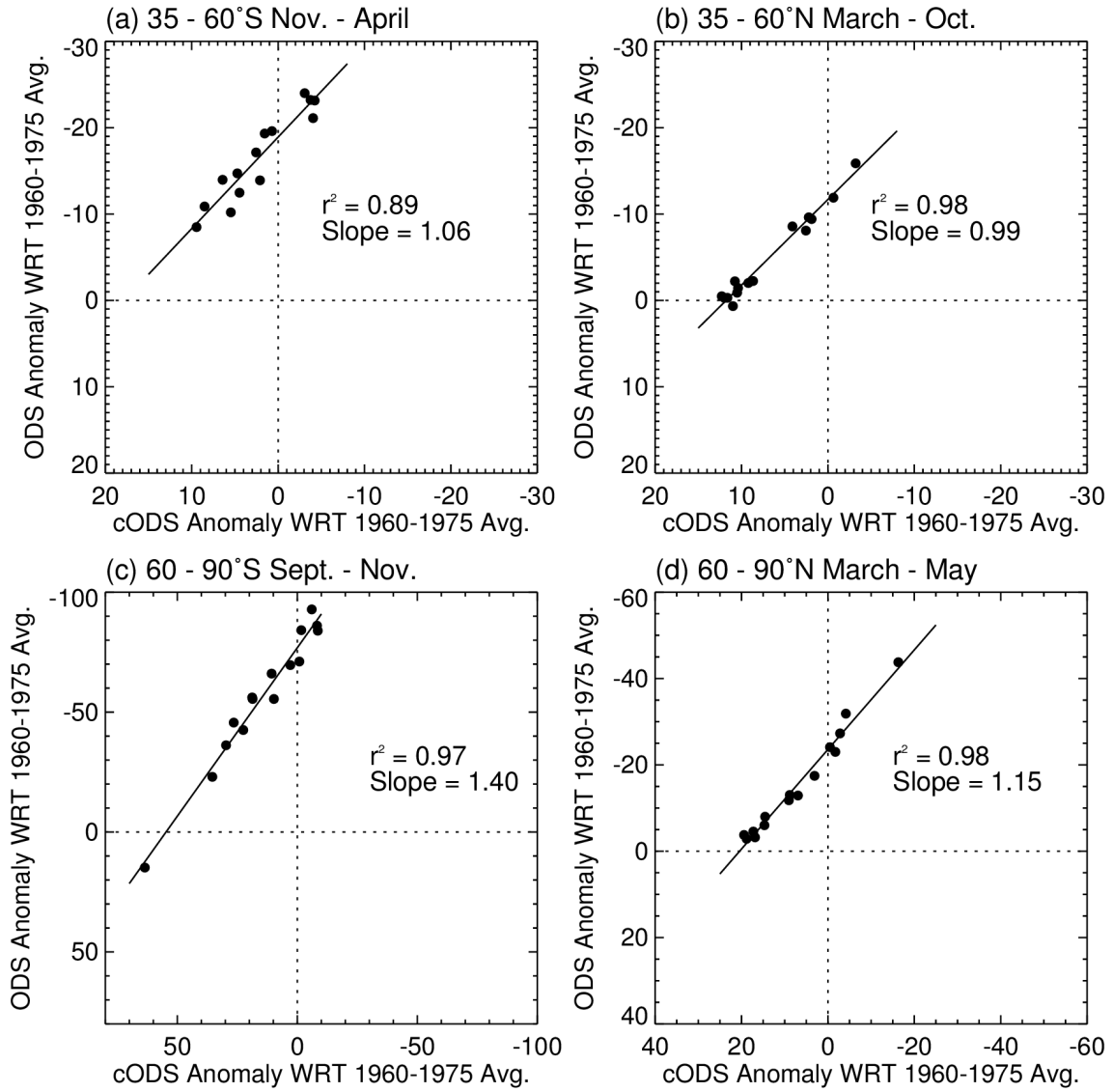
1 **Figure 3**



2

3

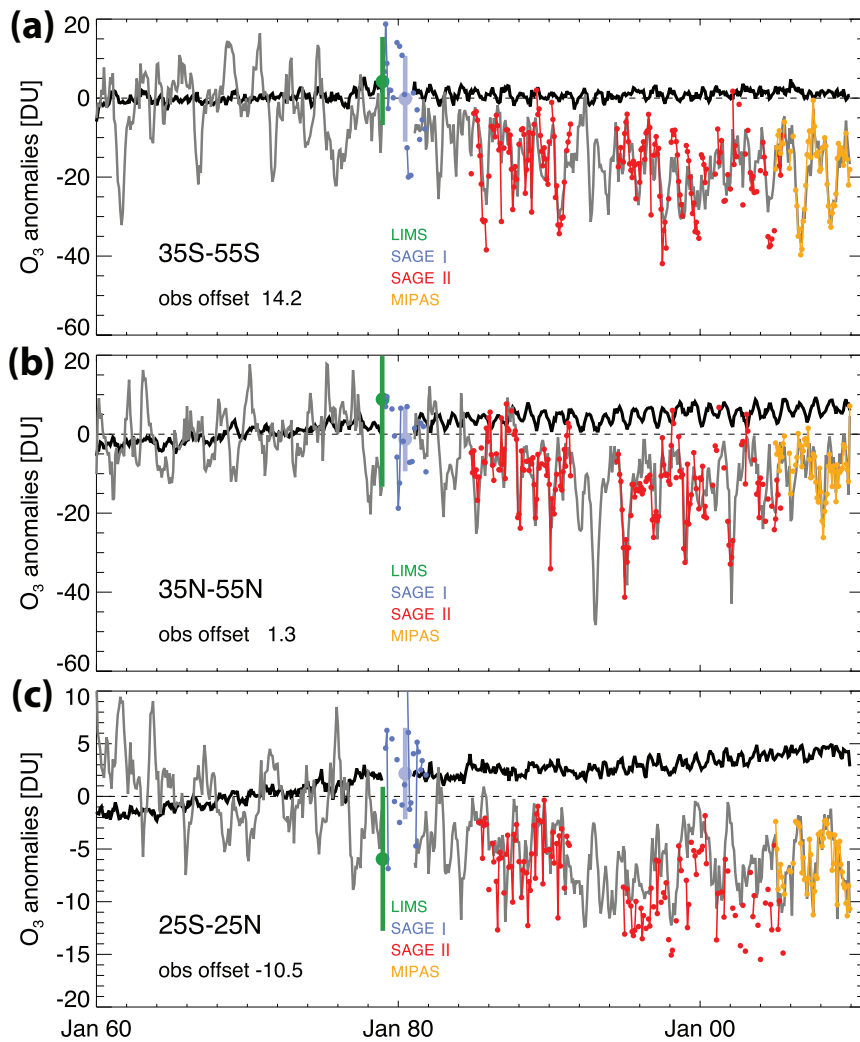
1 **Figure 4**



2

3

1 **Figure 5**



2

3

1 **Table 1**

	60°S-60°N		25°S-25°N		35°N-60°N		35°S-60°S	
	DU	%	DU	%	DU	%	DU	%
Obs	-7.03 +/- 1.42	-2.41 +/- 0.49	-2.13 +/- 2.57	-0.81 +/- 0.98	-11.6 +/- 4.11	-3.36 +/- 1.19	-18.8 +/- 4.18	-5.84 +/- 1.30
ODS run	-6.56 +/- 1.13	-2.23 +/- 0.38	-2.34 +/- 1.81	-0.90 +/- 0.70	-6.79 +/- 4.79	-1.97 +/- 1.39	-18.0 +/- 5.87	-5.22 +/- 1.70
ODS strat	-9.45 +/- 0.95	-3.56 +/- 0.36	-5.24 +/- 1.71	-2.23 +/- 0.73	-11.6 +/- 4.34	-3.74 +/- 1.49	-18.6 +/- 5.23	-5.91 +/- 1.66
ODS trop	+2.89 +/- 0.78	+9.98 +/- 2.69	+2.91 +/- 0.69	+12.0 +/- 2.84	+4.82 +/- 1.47	+13.7 +/- 4.18	+0.57 +/- 1.19	+1.88 +/- 3.90
cODS run	+2.72 +/- 1.15	+0.92 +/- 0.39	+3.50 +/- 1.86	+1.34 +/- 0.71	+4.35 +/- 5.12	+1.25 +/- 1.47	-0.54 +/- 5.34	-0.15 +/- 1.54
cODS strat	-1.45 +/- 0.99	-0.54 +/- 0.37	-0.27 +/- 1.78	-0.11 +/- 0.75	-1.45 +/- 4.95	-0.46 +/- 1.59	-3.66 +/- 4.77	-1.15 +/- 1.51
cODS trop	+4.17 +/- 0.82	+14.3 +/- 2.80	+3.77 +/- 0.71	+15.5 +/- 2.93	+5.79 +/- 1.50	16.4 +/- 4.26	+3.12 +/- 1.20	+10.2 +/- 3.91
ODS-cODS	-9.28 +/- 0.59	-3.15 +/- 0.20	-5.84 +/- 0.46	-1.98 +/- 0.16	-11.1 +/- 0.88	-3.78 +/- 0.30	-17.5 +/- 0.94	-5.94 +/- 0.32
ODS-cODS strat	-8.00 +/- 0.57	-3.02 +/- 0.21	-4.98 +/- 0.44	-1.88 +/- 0.17	-10.2 +/- 0.86	-3.83 +/- 0.32	-14.9 +/- 0.88	-5.62 +/- 0.33
ODS-cODS trop	-1.28 +/- 0.05	-4.42 +/- 0.19	-0.86 +/- 0.04	-2.96 +/- 0.14	-0.97 +/- 0.05	-3.35 +/- 0.18	-2.55 +/- 0.14	-8.78 +/- 0.48

2

3

Reconciling halogen-induced ozone loss with the observed total ozone record

T.G. Shepherd, D.A. Plummer, J.F. Scinocca, M.I. Hegglin, V.E. Fioletov, M.C. Reader, E. Remsberg, T. von Clarmann, H.J. Wang

Bridging the ERA-40/ERA-Interim transition. For the model simulations, there is a potential inhomogeneity between the ERA-40 and ERA-Interim portions of the record which if not corrected could introduce spurious long-term changes in the modelled ozone. The cODS simulation is used to identify the effect of this inhomogeneity because the stratospheric ozone changes in the cODS simulation are relatively small; since the inhomogeneity affects both the cODS and ODS simulations in the same way (as confirmed by the smoothness of the ODS-cODS differences across the 1979 transition, see Figure 3), adjustments made to the cODS simulation can also be applied to the ODS simulation, producing a homogeneous record. Figure S1 shows the stratospheric and tropospheric ozone timeseries for various regions. For the stratospheric timeseries, there are no trends evident in the cODS simulation during either the ERA-40 or ERA-Interim portions of the record, thus no trend is assumed between them and a constant offset is applied to the ERA-Interim portion of the record so that the average monthly mean values over the 1964-1978 and 1981-1995 periods (shown by the horizontal lines, with uncertainties) match. It is clear from the figure that determining the offset from the ODS simulation would be

far more difficult because of the ODS-induced trends. For the tropospheric cODS timeseries, trends are evident during both parts of the record (consistent with changes in tropospheric emissions of ozone precursors), so a constant offset to the ERA-Interim portion of the record is applied such that the linear trends in the monthly mean values over the 1960-1978 and 1981-2009 periods (shown by the straight lines, with uncertainties) meet in 1980. The uncertainties in these offsets are propagated through to the uncertainties in the long-term changes shown in Table 1. Note that the offsets only affect ozone changes between the pre-1979 and post-1979 periods, not changes within either period; nor do they affect the cODS-ODS differences. A transition period of a few years is evident in the raw timeseries following the switch to ERA-Interim in 1979, hence the adjusted timeseries shown in Figures 1, 2 and 5 are not plotted between 1979 and 1981.

Definitions of confidence intervals. The 95% confidence intervals (CIs) of the total column ozone differences were calculated from the standard error of the means assuming the errors are distributed as Student's t. Since the differences in total column ozone implicitly contain the offsets used to merge the ERA-40 and ERA-Interim periods of the simulation, the standard errors of the offsets were added in quadrature to the standard errors of the means. The standard errors of the offsets were, in turn, calculated from the standard errors of the mean stratospheric column of the cODS experiment over 1964-1978 and 1981-1995 and the standard error on the linear least-squares fit to the tropospheric ozone column at 1980. The standard error in the linear regression of the tropospheric column accounts for the

1 extrapolation of the 1960-1978 linear trend forward to 1980 and the extrapolation
2 backwards to 1980 of the linear trend calculated over 1981-2009. Noting that the
3 mean over the 1964-1978 period appears as a term both in the calculation of the
4 ERA-40/ERA-Interim offset and in the 1964-1978 to 1996-2002 differences given in
5 Table 1, and that the interannual variability in the ODS and cODS experiments was
6 essentially identical over this period, the contribution of the standard error of the
7 1964-1978 mean cancelled out in the calculation of the CI for the stratospheric and
8 total column ozone changes. The calculation of the 95% CI for the stratospheric
9 column differences was verified by comparing the CI with that derived by a Monte
10 Carlo method where the data for 1964-1978, 1981-1995 and 1996-2002 were
11 resampled with replacement 10000 times and the ERA-40/ERA-Interim offset and
12 column differences were recalculated for each sample. The effective sample size for
13 all quantities was adjusted to account for the lag-1 autocorrelation.

14

15

1 **Figure S1 | Determination of offsets between ERA-40 and ERA-Interim periods.**

2 Original time series of cODS (black) and ODS (red) simulations for each of the four
3 latitude bands (35-60N, 25S-25N, 35-60S, 60S-60N), for both tropospheric and
4 stratospheric ozone. Linear trends in the cODS simulation over the periods 1964-
5 1978 and 1981-1995 are indicated within each panel. Within each subregion, the
6 stratospheric trends are not statistically distinguishable from zero, hence are
7 assumed to be zero and the mean values over each period are computed (shown as
8 black horizontal lines with 95% confidence intervals); their difference determines
9 the offset, which is indicated within each panel. Non-zero tropospheric trends are
10 clearly present, so in this case a linear fit is made to each time period (straight black
11 lines with 95% confidence intervals); the difference between those fits in 1980
12 determines the offset, which is indicated within each panel.

13

